Twisted intramolecular charge transfer states: Rotationally resolved fluorescence excitation spectra of 4,4′-dimethylaminobenzonitrile in a molecular beam

A. E. Nikolaev
Department of Chemistry, University of Pittsburgh, Pittsburgh, Pennsylvania 15260

G. Myszkiewicz, G. Berden,[a)] and W. Leo Meerts[b)]
Department of Molecular and Laser Physics, Institute for Molecules and Materials, Radboud University Nijmegen, P.O. Box 9010, 6500 GL Nijmegen, The Netherlands

J. F. Pfanstiel[c)] and D. W. Pratt[d)]
Department of Chemistry, University of Pittsburgh, Pittsburgh, Pennsylvania 15260

We report the observation at high resolution of seven vibronic bands that appear within ~ 200 cm^{-1} of the electronic origin in the S_1-S_0 fluorescence excitation spectrum of 4,4′-dimethylaminobenzonitrile (DMABN) in a molecular beam. Surprisingly, each band is found to be split into two or more components by a (coordinated) methyl group tunneling motion which significantly complicates the analysis. Despite this fact, high quality [(Observed–Calculated) ≤ 30 MHz] fits of each of the bands have been obtained, from which the rotational constants, inertial defects, torsion-rotation interaction constants, methyl group torsional barriers, and transition moment orientations of DMABN in both electronic states have been determined. The data show that DMABN is a slightly pyramidalized ($\sim 1°$) but otherwise (heavy-atom) planar molecule in its ground S_0 state, and that its electronically excited S_1 state has both a more pyramidalized ($\sim 3°$) and twisted ($\sim 25°$) dimethylamino group. Large reductions in the methyl group torsional barriers also show that the $S_1 \leftarrow S_0$ electronic transition is accompanied by significant charge transfer from the nitrogen atom to the π^* orbitals of the aromatic ring. Thereby established is the participation of all three vibrational coordinates in the dynamics leading to the "anomalous" emissive behavior of DMABN in the condensed phase. © *2005 American Institute of Physics.* [DOI: 10.1063/1.1850092]

I. INTRODUCTION

Literally hundreds (if not thousands) of publications have appeared in the past 50 years concerning the properties of 4,4′-dimethylaminobenzonitrile (DMABN) and related molecules in their ground and electronically excited states. Mainly, this is because of its "anomalous" emission spectrum in the condensed phase. In addition to the normal fluorescence that is always present, DMABN exhibits an additional, redshifted emission in polar solvents that was first attributed by Lippert *et al.*[1] to an intramolecular charge transfer (ICT) state. Later, recognizing that charge separation and/or flow would be inhibited by orbital overlap between the two ends of the molecule, Grabowski and co-workers[2] suggested that the process involved an internal twisting of the dimethylamino (DMA) group. Such a motion would facilitate "permanent" transfer of electrons from the amino nitrogen to a π^* orbital extending over the aromatic ring. This hypothesis, leading to the concept of twisted intramolecular charge transfer (TICT) states, was then tested in an extensive series of experiments by Grabowski, Rotkiewicz, Rettig, and many others.[3] In the following years, other competing models of structural relaxation were proposed, including the so-called planar ICT (PICT) model advocated by Zachariasse and co-workers.[4,5]

Despite the passage of time, the intense controversy generated by these proposals, and the extensive application of ICT molecules as fluorescence markers, sensors, and "switches" in materials science and in biology, very little is known about their electronic and geometric structures. Gas phase, fluorescence excitation spectra of DMABN in supersonic jets were first reported by Kobayashi *et al.*,[6] Gibson *et al.*,[7] and Bernstein and co-workers.[8] Significant activity of several vibrational modes lying within the first 200 cm^{-1} of the origin was detected in both the excitation and emission spectra and attributed to both DMA inversion and twisting motions. Kajimoto *et al.*[9] measured the microwave spectrum of DMABN and found the ground state to be nearly planar with an inversion angle of about 15°. They also observed a partially resolved rotational band contour of the S_1-S_0 electronic spectrum of DMABN and concluded that, in the S_1 state, the DMA group is rotated by 30° from the aromatic plane. Salgado *et al.*[10] reported on the basis of similar laser experiments on the isolated molecule that the laser-induced fluorescence (LIF) spectrum contained two types of con-

a)Present address: FOM Institute for Plasma Physics "Rijnhuizen," Edisonbaan 14, 3439 MN Nieuwegein, The Netherlands.
b)Electronic mail: leo.meerts@science.ru.nl
c)Present address: Bettis Atomic Power Laboratory, P.O. Box 79, West Mifflin, Pennsylvania 15122.
d)Electronic mail: pratt@pitt.edu

122, 084309-1

tours, *b*-type bands that belonged to a "planar" excited state and *c*-type bands that belonged to a "twisted" excited state. But Saigusa *et al.*[11] suggested on the basis of a reexamination of the low resolution spectra of DMABN-h_6 and -d_6 that all bands terminate in an S_1 state that is twisted by about 26° with a small 150 cm^{-1} barrier to planarity. The structural and dynamical behaviors of S_1 DMABN also have been the subject of many theoretical calculations, most recently using TDDFT methods.[12]

Reported here are the results of rotationally resolved fluorescence excitation experiments on DMABN in a molecular beam. The data give information about the equilibrium geometry of the molecule in its ground electronic state, about the equilibrium geometry of the molecule in its excited electronic state, and about the differences in the electronic distributions of the two states. Studies of seven different vibronic bands in the S_1-S_0 spectrum show that DMABN is an essentially planar molecule in its S_0 state, that it is a slightly pyramidal, significantly twisted molecule in the S_1 state, and that significant charge transfer is facilitated by vibrational motion along these coordinates. Thereby established is a direct connection between the properties of the isolated molecule and its behavior in the condensed phase.

II. EXPERIMENT AND ANALYSIS

DMABN was purchased from Aldrich and used without further purification. Low resolution experiments to determine the frequencies of the transitions for subsequent examination at high resolution were performed as described elsewhere.[13] The high resolution data were obtained using two molecular beam laser spectrometers.[14,15] The sample was heated to about 150 °C, seeded into 500 torr of argon, expanded through a 150 μm quartz nozzle, skimmed once, and crossed 15 cm downstream of the nozzle by a single frequency, tunable visible laser, intracavity frequency doubled into the UV. Reduction of the Doppler width to ≈20 MHz was accomplished by active control of the angle between the laser and molecular beams, which was as close to 90° as possible, and by spatially selective detection optics, which collects light from a ~0.7 mm diameter sphere located at the center of the crossing point. The laser is a Spectra-Physics Ar$^+$-pumped ring dye laser (Models 171 and 380D) that has been modified for intracavity frequency doubling and extended tuning over ranges (in the UV) of up to 7 cm^{-1}. The homogeneous linewidth of the laser is less than 1 MHz. In a typical experiment, the laser was scanned across the width of a single band, producing fluorescence at selected wavelengths that was detected by a photomultiplier tube and photon-counting system and processed by a computer-controlled data acquisition system. As will be seen, each spectrum consists of thousands of lines which connect the populated rotational levels of the ground state with the corresponding, accessible rotational levels of the excited electronic state.

The spectra were analyzed using the effective Hamiltonian for an asymmetric molecule with two equivalent CH$_3$ internal rotors discussed by Tan *et al.*[16] An extensive initial search for the best fit parameters for each of the spectra was performed with the automated assignment technique based
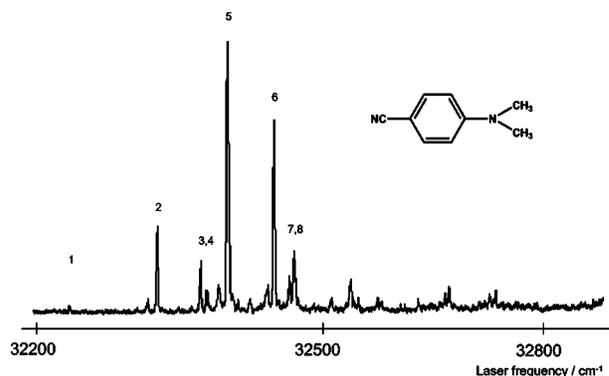
on genetic algorithms (GA) developed in Nijmegen.[17,18] These results were then subsequently used to perform line assignments with Plusquellic's program[19] JB95 and a detailed fit of these assignments to the effective Hamiltonian. *Ab initio* calculations were performed using GAUSSIAN 98.[20]

III. RESULTS

Figure 1 shows the low resolution fluorescence excitation spectrum of DMABN. Similar to the spectra recorded by others,[6–8] the spectrum has a weak origin band at ~32 247 cm^{-1} but exhibits many strong features within the first 200 cm^{-1} of the origin. These have been assigned most recently by Saigusa *et al.*[11] as involving DMA torsional, DMA inversion, and methyl torsional motions. These assignments are listed in Table I. Similar low frequency activity is built on higher energy vibronic transitions displaced by ~600 cm^{-1}, etc., from the origin, as in the case of other substituted benzenes. Thus, apart from this low frequency activity, the S_1 state of DMABN in the gas phase appears to be a normal, locally excited $\pi\pi^*$ state of a typical aromatic molecule.

To date, our high resolution study has been confined to the seven strongest bands in the first low frequency progression. The origin band proved too weak to record under the present conditions. Figure 2 shows the rotationally resolved

FIG. 1. Vibrationally resolved fluorescence excitation spectrum of DMABN.

TABLE I. Observed vibrational bands in the $S_1 \leftarrow S_0$ fluorescence excitation spectrum of 4,4′-dimethylaminobenzonitrile (DMABN).

Band	Band origin (cm^{-1})[a]	Displacement from origin (cm^{-1})	Assignment[b]	ΔI avg, amu Å^2[c]
1	32 246.73	0	Origin	(Not observed)
2	32 322.33	75.6	τ_0^2	−12.27
3	32 360.15	113.4	I_0^2	−12.50
4	32 365.60	118.9	$\tau_0^1 Mh_0^1$	−14.22
5	32 383.37	136.6	τ_0^4	−11.47
6	32 423.64	176.9	τ_0^6	−11.93
7	32 436.92	190.2	$\tau_0^2 I_0^2$	−13.46
8	32 440.77	194.0	$\tau_0^3 Mh_0^1$	−12.11

[a]Calculated from the observed *G*-*G* subband origin frequency (Table II).
[b]S_1 vibrational levels that participate in the indicated transition. τ denotes DMA torsion, I denotes DMA inversion, and Mh denotes methyl torsion. See Ref. 11.
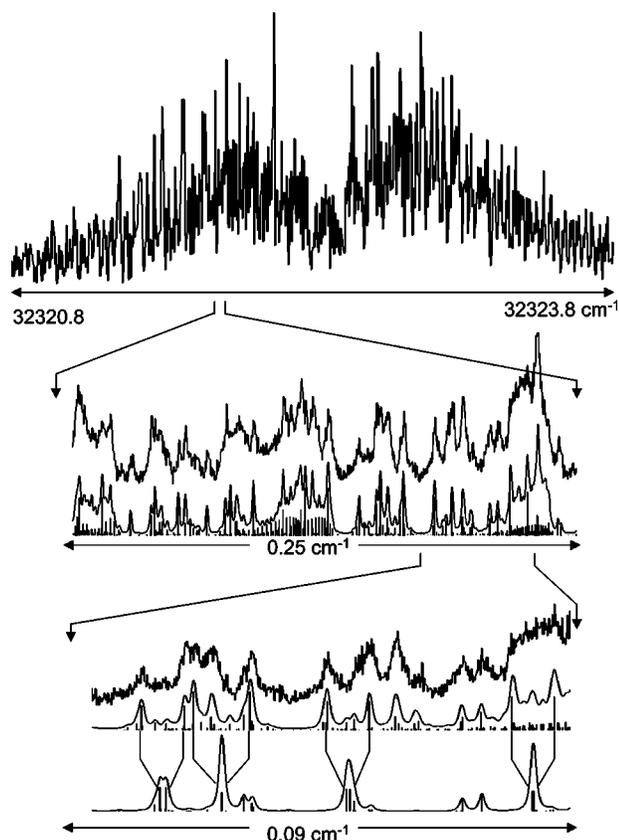[c]Average values for all subbands lying within the indicated band.

FIG. 2. Rotationally resolved fluorescence excitation spectrum of Band 2 in DMABN. Shown in the middle is a small portion of the experimental spectrum, the fitted spectrum with a convoluted line shape function, and the individual lines of the separate subbands that contribute to the spectrum in this region. Illustrated at the bottom is a still smaller portion of the spectrum showing the first-order torsion-rotation splittings for (left to right) transitions $[J'K_a'K_c'–J''K_a''K_c''] = [10\ 3\ 8–11\ 4\ 7]$, $[4\ 4\ 1–5\ 5\ 0]$, $[9\ 3\ 7–10\ 4\ 6]$ and $[8\ 3\ 5–9\ 4\ 6]$. Among the splittings shown, the one involving the degenerate pair $[441–550]$ and $[440–551]$ is the largest.

spectrum of Band 2, located at 32 322 cm^{-1} (+76 cm^{-1}). The entire spectrum contains in excess of 3000 lines and spans over 3 cm^{-1} at a rotational temperature of 4 K. Initial attempts to fit this spectrum showed that it contains at least two closely spaced subbands with similar inertial parameters.[21] A weak third subband was discovered in refinements of the fit with the computer assisted GA. Thus, it was determined that three distinct rotational contours, separated by ~3 GHz and having relative intensities of ~1:2:1, comprise Band 2. There are ≈1000 lines in each subband.

Refined values of the rotational constants of the two states that participate in Band 2 were obtained by first fitting the strong subband. A simulated spectrum of this subband was generated using the previously measured rotational constants of the ground state[9] and CIS 6-31+G values for the excited state. This was sufficient to reproduce its main features. Then, assisted by the GA results, "copies" of this spectrum were shifted to the approximate origins of the two remaining subbands until their main features were reproduced as well. Assignments of several transitions in each of the subbands were then made and refined values of the rotational constants were obtained, using a least squares fitting procedure.

An important result of this exercise was the discovery that only one of the three subbands, the lowest frequency one, could be fit using rigid rotor Hamiltonians for both states. The two higher frequency bands required the addition of terms linear in the angular momentum quantum numbers to the Hamiltonian of the excited state. As discussed elsewhere,[16] terms of this sort arise from the coupling of overall rotation with other sources of angular momentum, such as internal rotation. The principal experimental evidence for this conclusion are splittings observed in some of the lines, especially those connecting levels having K_a nearly equal to J. These transitions are near degenerate in the case of near prolate asymmetric rotor. However, addition of linear terms to the Hamiltonian removes this degeneracy. A specific example from the strong subband is shown in Fig. 2, where two fits, with and without linear terms, are compared.

The final fit of Band 2 utilized 198 assigned lines for the first subband, 333 lines for the second subband, and 91 lines for the third subband, with standard deviations of 10.7, 8.1, and 20.1 MHz, respectively. One possible explanation for the high OMC (Observed–Calculated) value of the third subband is the high density of lines and low signal-to-noise. Another is that this subband (the E subband) is predicted to consist of two overlapping transitions (the E_1+E_3 subbands).[16] For this reason, we also fit the entire spectrum using GA and the model Hamiltonian, completely reproducing the entire spectrum. The inertial constants derived from the two fits were the same, within experimental error.

All subbands in Band 2 are mainly b-type bands. Owing to band congestion, the possible contributions of other band types could not be determined. The resulting inertial constants of both ground and excited state are accurate to at least ±1 MHz. The ground state values compare favorably with the earlier microwave values.[9] Typically, microwave values are more precise, but in this case only eight pure rotational transitions were measured, making the precision in our experiment at least as high as the microwave one. Individual lines identified in the fitting process have full widths at half maxima of about 50 MHz. Examination of the individual line shapes suggests approximately equal contributions to them from Doppler and lifetime broadening. The 5 ns fluorescence lifetime measured for DMABN in the gas phase by Howells *et al.*[22] suggests a Lorentzian contribution to the linewidth of 32 MHz. The results for Band 2 are summarized in Tables II and III, which separately list the ground and excited state parameters of all seven studied bands of DMABN. The results for the E subbands are not reported here owing to their high OMC values. Standard deviations increase for the lower intensity subband fits, as the number of readily assignable transitions is smaller.

Figure 3 shows the rotationally resolved spectra of the remaining six bands, Bands 3–8. Band 3, observed at ~32 360 cm^{-1} (+113 cm^{-1}), contains more than 2000 lines and, even though it appears to be a b-type band (no obvious Q branch), one can immediately see that there is significant intensity in the region where a Q branch would have been expected. This prompted us again to look for the presence of subbands. Using procedures similar to those described above, it was determined that three subbands are present in

TABLE II. Ground state inertial parameters derived from fits of Band 2–8 in the S_1-S_0 electronic spectrum of DMABN. All parameters in MHz, except for ΔI (amu Å^2).

Band	A	B	C	ΔI	Origin frequency
2 *A-A*	3470.3(4)	578.7(3)	499.6(1)	−7.41(40)	968 995 908
G-G	3470.5(5)	578.6(2)	499.5(1)	−7.46(20)	+3052.6
3 *A-A*	3470.0(5)	578.6(1)	499.7(1)	−7.76(20)	970 118 243
G-G	3470.0(5)	578.6(1)	499.7(1)	−7.75(20)	+14 702
4 *A-A*	3468.9(8)	578.6(3)	499.5(2)	−7.34(40)	970 296 024
G-G	3469.6(5)	578.6(2)	499.6(2)	−7.59(40)	+372.4
5 *A-A*	3469.3(10)	578.6(2)	499.6(1)	−7.49(30)	970 814 803
G-G	3469.4(20)	578.6(2)	499.5(1)	−7.47(30)	+14 250
6 *A-A*	3470.9(8)	578.8(1)	499.8(1)	−7.57(20)	972 035 675
G-G	3471.0(8)	578.8(1)	499.7(1)	−7.57(15)	+524.5
7 *A-A*	3471.2(7)	578.8(1)	499.8(1)	−7.63(20)	972 422 232
G-G	3471.4(7)	578.9(1)	499.9(1)	−7.56(20)	+12 092
8 *A-A*	3470.6(6)	578.8(1)	499.8(1)	−7.64(15)	972 522 977
G-G	3470.5(6)	578.8(1)	499.8(1)	−7.57(15)	+26 814

Band 3, separated by ∼15 GHz with relative intensities of ∼2:5:3 and linewidths comparable to those in Band 2. The final fit of Band 3 utilized 41 assigned lines for the first subband, 369 lines for the second subband, and 75 lines for the third subband, with standard deviations of 19.8, 5.0, and 13.1 MHz, respectively. A contour GA fit again reproduced the spectrum of the third subband.

The rotationally resolved spectrum of Band 4, observed at ∼32 366 cm^{-1} (+119 cm^{-1}), has a different appearance. It is significantly more congested than Bands 2 and 3. This is due to the presence of three closely spaced subbands, separated by ∼370 MHz, with relative intensities of ∼2:6:3. As in the previous cases, we attempted to fit the spectrum with rigid rotor Hamiltonians for both electronic states. However, as before, it was required to introduce linear terms into the excited state Hamiltonian of the two higher frequency subbands. The final fit of Band 4 utilized 52 assigned lines for the first subband, 272 lines for the second subband, and 137 lines for the third subband, with standard deviations of 8.5, 11.3, and 7.9 MHz, respectively.

TABLE III. Excited state inertial parameters derived from fits of Bands 2–8 in the S_1-S_0 electronic spectrum of DMABN. All parameters in MHz, except for ΔI (amu Å^2).

Band	A	B	C	D_a	D_b	ΔI
2 *A-A*	3405.6(4)	575.5(3)	498.2(2)	…	…	−12.19(30)
G-G	3405.0(5)	575.3(2)	498.1(2)	42.4(30)	24.5(400)	−12.34(20)
3 *A-A*	3374.5(1)	576.8(1)	498.4(5)	…	…	−12.00(30)
G-G	3396.2(5)	575.6(1)	498.5(1)	186.0(3)	44.6(200)	−12.99(20)
4 *A-A*	3374.7(7)	576.0(3)	498.8(2)	…	…	−14.07(40)
G-G	3375.8(7)	576.0(2)	499.0(1)	7.0(3)	0	−14.36(30)
5 *A-A*	3400.1(10)	576.3(2)	498.4(1)	…	…	−11.69(40)
G-G	3394.6(20)	576.4(1)	498.1(1)	305.4(5)	28.2(20)	−11.25(10)
6 *A-A*	3401.4(7)	575.7(1)	498.3(1)	…	…	−12.17(10)
G-G	3401.3(5)	576.1(1)	498.3(1)	118(3)	10(30)	−11.68(10)
7 *A-A*	3394(3)	576.6(1)	499.2(1)	…	…	−12.87(10)
G-G	3383.1(5)	576.4(1)	499.3(1)	192.4(2)	37(20)	−14.04(20)
8 *A-A*	3407.3(5)	576.5(1)	498.8(1)	…	…	−11.87(10)
G-G	3397.7(1)	576.3(1)	498.7(1)	554(4)	82.4(8)	−12.34(20)

Band 5, observed at ∼32 383 cm^{-1} (+136 cm^{-1}), is the strongest band in the studied frequency range and was obtained with the highest signal-to-noise. Despite this fact, lines of only two subbands could be assigned. These bands are separated by ∼14 GHz with a relative intensity of ∼1:2. It was sufficient to use rigid rotor Hamiltonians for the ground and excited states of the lower frequency subband, while some linear terms were required to fit the stronger, higher frequency subband. The final fit of this spectrum was based on the assignment of 112 lines for the first subband and 114 for the second, with standard deviations of 3.9 and 4.5 MHz, respectively. A GA fit of the full spectrum showed the presence of a third subband shifted another ∼14 GHz to the blue.

Band 6, observed at ∼32 424 cm^{-1} (+177 cm^{-1}), is the second strongest band in the studied frequency range and is similar in all respects to Band 5 (cf. Fig. 3). At first glance, Band 6 appears to contain two subbands with relative intensity of ∼1:2. In this case, the spacing of two subbands is ∼500 MHz. Analogous to Band 5, the lower intensity (low frequency) subband in Band 6 could be fit using only rigid rotor Hamiltonians for both states, while the higher intensity subband required introduction of linear terms in the Hamiltonian of the excited state. The fit was based on 78 assignments for the first subband and 206 assignments for the second subband, with standard deviations of 2.9 and 1.5 MHz, respectively. A GA fit pointed to the existence of a third subband at still higher frequency about 500 MHz to the blue.

Band 7, observed at ∼32 437 cm^{-1} (+190 cm^{-1}), appears to again contain only two subbands, split by ∼12 GHz with a relative intensity of ∼4:7. 324 lines were assigned for the weaker subband and 225 for the stronger one, with standard deviations of 2.8 and 2.1 MHz, respectively. The lower intensity subband was fit using only rigid rotor terms in the Hamiltonian. The higher intensity subband contained characteristic internal rotation splittings, analogous to those observed in other bands, which required the addition of linear terms to the Hamiltonian of the excited state. A third subband was again shown to be present in Band 7 by the GA fit.

The rotationally resolved spectrum of Band 8 was observed at ∼32 441 cm^{-1} (+194 cm^{-1}). Band 8 was initially identified as *b* type, with no apparent splittings. Only after the initial fit was performed, using a Hamiltonian with internal rotation terms in the excited state, was significant additional intensity observed in the lower frequency portion of the spectrum. This new intensity was accounted for by the introduction of a second subband, shifted by an unprecedented ∼27 GHz to the red, with relative intensity of ∼1:2. 196 lines were assigned for the lower intensity subband and 162 lines were assigned for the higher intensity subband, resulting in standard deviations of the fit of 2.2 and 2.4 MHz, respectively. The remaining intensity in the highest frequency part of the spectrum (not shown in Fig. 3) could be attributed to a third subband with a GA calculation.

It is important to note at this juncture that each of the rotational constants listed in Tables II and III contains second-order contributions due to the torsion-rotation interaction. However, from an estimate of the torsional barriers (*vide infra*), it can easily be shown that these contributions
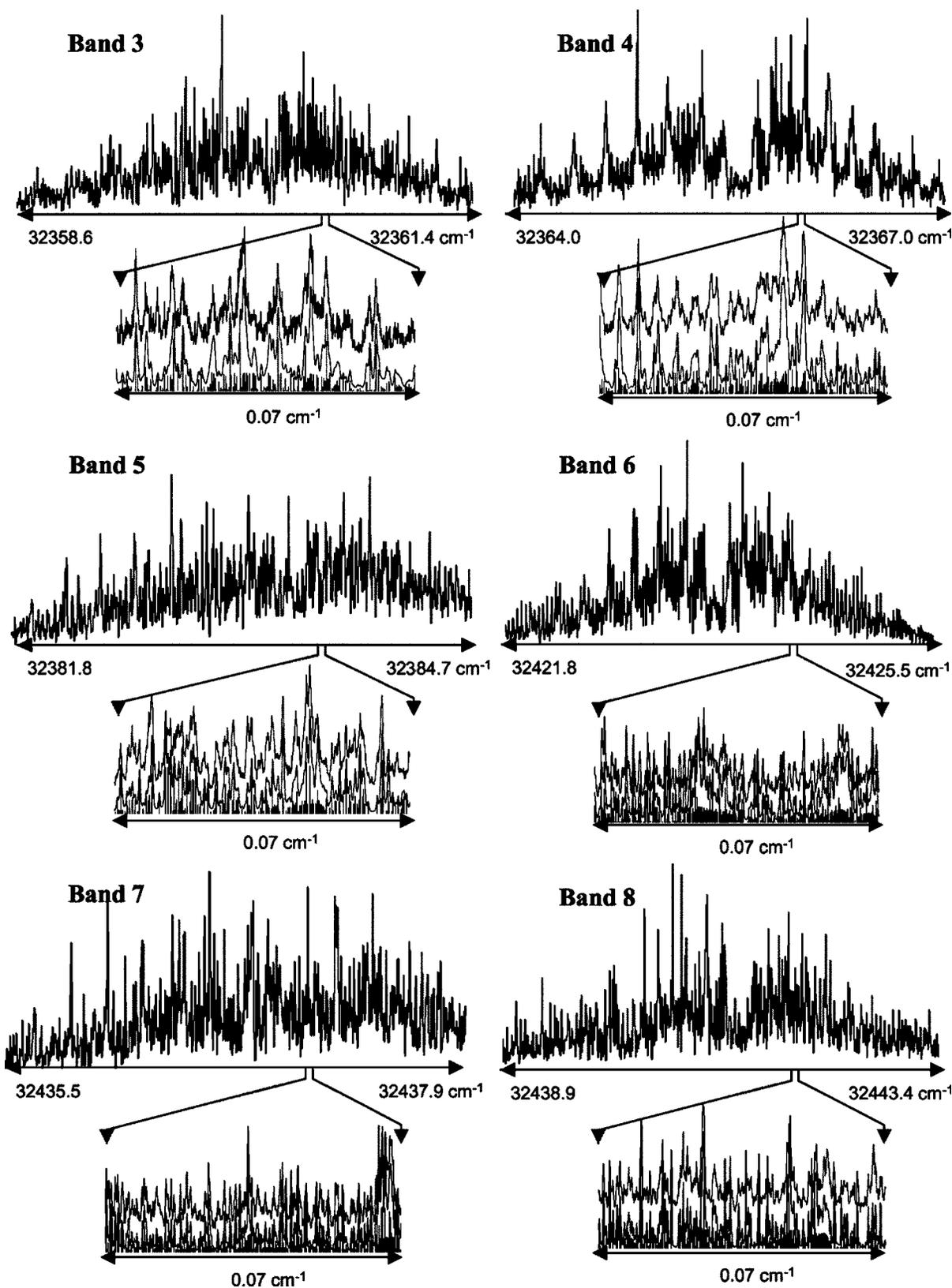
FIG. 3. Rotationally resolved fluorescence excitation spectra of Bands 3-8 in the S_1-S_0 electronic transition of DMABN.

are small, of the order 0.01 MHz or less (except for the excited state level involved in Band 8, where they approach 10 MHz). Therefore, they are neglected in what follows. We also reiterate here that all studied Bands 2–8 are b-type bands and exhibit the same single rovibronic linewidths,

50 MHz or so. This demonstrates that these bands all access upper state vibrational levels which have comparable lifetimes.

The band origin frequencies presented in Table I are from the G-subband origins of the high resolution spectra

TABLE IV. Calculated and observed inertial parameters of DMABN in its ground and electronically excited states.

	Parameter	Experiment (average values)	MW[a]	HF/6-31+G	Fit
S_0	A, MHz	3470.3[b]	3470.0	3499.1	3487.7[c]
	B, MHz	578.7[b]	578.6	580.5	583.6[c]
	C, MHz	499.7[b]	499.6	501.0	503.7[c]
	ΔI, amu Å^2	−7.56[b]	−7.36	−6.28	−7.54[c]
				CIS/6-31+G	
S_1	A, MHz	3405.6[d]		3395.6	3395.4[e]
	B, MHz	575.5[d]		578.8	577.4[e]
	C, MHz	498.2[d]		497.5	499.1[e]
	ΔI, amu Å^2	−12.19[d]		−6.14	−11.58[e]

[a]Microwave values (Ref. 9).
[b]Average values for all subbands.
[c]Modified theoretical structure of ground state with inversion angle=18.5°, CNC angle=122°.
[d]Values for the A subband in Band 2.
[e]Modified theoretical structure of excited state with twist angle=25°, inversion angle=30°.

from Table II. These are the best numbers for the low resolution spectra since the weighted intensity of the A, G, and E subbands coincides exactly with the origin of the G subband.

IV. DISCUSSION

A. Structural considerations

Examination of the ground state rotational constants in Table II reveals that the values of A, B, and C of Bands 2–8 are all the same, within experimental error. This shows that all seven bands originate in the same vibrational level of DMABN, presumably the zero-point level of its S_0 state. The different transitions cannot be hot bands, nor can they belong to different conformers of DMABN. Each of these possibilities would require that the ground state rotational constants of the different bands be different.

To interpret these values, we first performed a number of theoretical calculations. At the HF/6-31+G level, DMABN converges to a "planar" structure; the CN group and the heavy atoms of the DMA group all lie in the aromatic plane. Importantly, this structure has significantly different inertial parameters from the observed one, as shown in Table IV. Planar DMABN has an inertial defect ($\Delta I = I_c - I_a - I_b$) of −6.28 amu Å^2 whereas the experimental structure has $\Delta I = -7.56$ amu Å^2. (This is the average value for all seven bands.) A large fraction of the observed inertial defect comes from the out-of-plane C–H bonds of the two methyl groups. For comparison, the inertial defect of 2,3-dimethylnaphthalene in its S_0 state is −6.55 amu Å^2.[16] But there must be at least one other out-of-plane contribution in DMABN.

Additional contributions to the inertial defect may originate from pyramidalization of the N atom or twisting of the DMA group. To distinguish these contributions, one may consider also the values of the A rotational constant. Twisting the DMA group of a flat DMABN does not affect this parameter but pyramidalization does. Thus, "best-fit" values of the degrees of pyramidalization and twist may be obtained
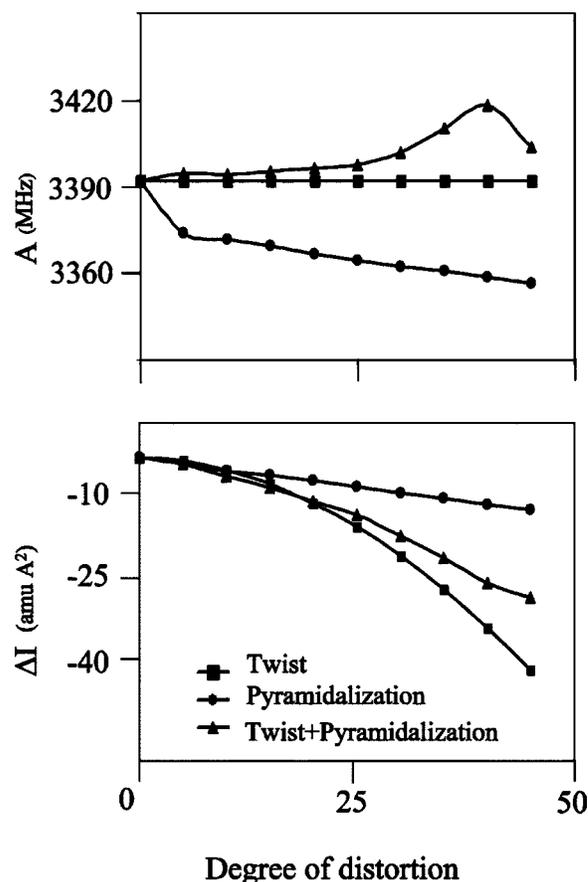

FIG. 4. Plots of the A rotational constant (in MHz, top) and inertial defect (in amu Å^2, bottom) of DMABN as a function of distortion along different vibrational coordinates (see legend).

by simultaneously changing them until the calculated values of A and ΔI match those of the experimental structure. No twist was necessary in the ground state. Pyramidalization of the DMA group by 1°, giving an inversion angle of 17.2°, yields a structure with $\Delta I = -7.36$ amu Å^2. Additional refinement is possible by varying the angle between methyl groups. Our best-fit structure has an inversion angle of 18.5° and an angle between the methyl groups of 122°, giving $\Delta I = -7.54$ amu Å^2 as shown in Table IV. Earlier microwave studies[9] estimated an inversion angle of 15°. The corresponding angle in the ground state of aniline is ~38°.[23]

Figure 4 shows a plot of the dependence of the inertial defect of DMABN on the inversion and twist angles of the DMA group. These data were obtained by distorting the HF/6−31+G structure along each coordinate, "freezing" the motion along all others, and calculating the changes in ΔI and A. The magnitude of ΔI increases along both coordinates. But, for reasonable values of both parameters, ΔI is much more sensitive to the torsional motion of the DMA group owing to the presence of the "off-axis" methyl groups.

Table III shows that the values of A, B, and C, and ΔI in the different excited state levels accessed in Bands 2–8 are mostly different, even among the different subbands accessed within a single band. As will be seen, these differences are significant, and provide key insights into the types of nuclear motion that are produced by the absorption of light. But, taken together, all values of A are about 2%

smaller in the S_1 state of DMABN whereas the values of B and C in the S_1 state are relatively unchanged, compared to the S_0 state. The values of the inertial defects in the S_1 state (ranging from -11 to -14 amu Å^2) are about 40% larger than that of the ground state. It is expected that aromatic molecules expand upon $\pi\pi^*$ excitation, which causes the overall decrease in rotational constants. The relatively large decrease in A indicates that the benzene ring is taking on a quinoidal shape as in the excited state of aniline.[23] However, elongation of the "perpendicular" bonds in the benzene ring cannot explain the larger (in magnitude) inertial defect values. This value is expected to remain unchanged at -6 to -7 amu Å^2.

While large, the decrease in the magnitude of A in S_1 DMABN is significantly smaller than that in S_1 aniline.[23] Aniline has $\Delta A \sim -331.2$ MHz, compared to $\Delta A \sim -65$ MHz in DMABN. 4-Aminobenzonitrile has $\Delta A = -316.6$ MHz.[24] While these are "smaller" molecules, with larger A values (aniline has $A = 5618$ MHz in the S_0 state), the *percent* change in A is also much larger in aniline and 4-aminobenzonitrile ($\sim 6\%$) than in DMABN ($\sim 2\%$).

To account for the smaller change in A, and for the large change in the magnitudes of the inertial defects in the S_1 state of DMABN, the contributions of pyramidalization and twist again have to be considered, as in the case of the ground state (cf. Fig. 4). Beginning with a planar DMABN, pyramidalization by at least $5°$ (giving an inversion angle of $\sim 38°$) is required to fit the observed values of ΔI. These angles are substantially larger than the corresponding angles in the ground state, which seems unreasonable to us. A "quinoidal" DMABN would have a flatter DMA group. Rotation of the DMA group by a twist angle of $17°$ with respect to the plane gives an inertial defect of -12.2 amu Å^2, in good agreement with experiment. (The A subband in Band 2 has $\Delta I = -12.19$ amu Å^2.) However, twist angles $\tau_{\min}$ of about $26°$ have been estimated from Franck–Condon fits of the vibrational progression in the low resolution spectrum.[11] Additionally, neither pyramidalization nor twisting the DMA group alone explains the relatively small ΔA value.

A unique solution to this problem is revealed only when one allows for *simultaneous* twisting and pyramidalization of the attached DMA group. Thus, starting with the modified *ab initio* structure of a hypothetical planar DMABN, the experimental values of *both* ΔI and A in the S_1 state can be fit by twisting the DMA group by $25°$ about the "C_2" axis *and* by pyramidalization of the nitrogen atom by $3°$. This is shown explicitly in Fig. 5. Such a coordinated motion is intuitively obvious on chemical grounds. If a "flatter" DMA group is a consequence of the conjugative interaction of the nitrogen lone pair π electrons and the electrons of the ring, then rotation of the DMA group with respect to the plane of this ring should reduce this interaction, and simultaneously allow for pyramidalization of the nitrogen atom. "Tetrahedral" nitrogen atoms are more stable than "trigonal" ones. Additionally, rotation of the DMA group also will produce a less quinoidal structure of the ring, since that structure also is a consequence of the same conjugative interaction. S_1 DMABN *must* have a significantly less quinoidal structure than S_1 aniline, given the difference in their ΔA values.
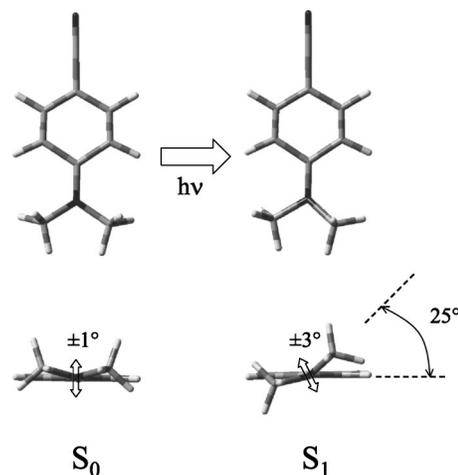

FIG. 5. The TICT state. Schematic diagram illustrating the geometry changes that occur when DMABN absorbs light.

B. The low resolution spectrum

That the DMA group is both twisted and pyramidalized in the S_1 state of DMABN also is apparent from its low resolution spectrum (Fig. 1). Saigusa *et al.*[11] have recently reexamined this spectrum in dimethylaniline, in DMABN, and in several of their isotopomers. They also have given compelling assignments of most of the observed bands appearing in this spectrum up to an excess energy of ~ 350 cm^{-1}. A key factor in these assignments was the discovery of the DMABN-d_6 origin band, which made possible a more meaningful comparison of the frequencies and intensities of the different bands in the different isotopomers. Based on these assignments, it was concluded that the prominent low frequency progression involves the DMA torsional mode, with less significant contributions from DMA inversion and methyl group torsional motions. The S_1 state was found to be twisted by about $26°$ with an effective twofold barrier of ~ 190 cm^{-1} at the planar configuration. An inversion angle of $15°$ was estimated for DMABN in its S_0 state (compared to $0°$ for the S_1 state). The corresponding angles in dimethylaniline were estimated to be $27°$ (S_0) and $13°$ (S_1).

Our results both confirm and extend the results of Saigusa *et al.*[11] Listed in Table I, in addition to the frequencies and displacements of the bands up to ~ 200 cm^{-1} above the origin of DMABN, are the proposed assignments and measured inertial defects of the S_1 vibrational levels that participate in these transitions. Here, τ denotes DMA torsion, I denotes DMA inversion, and Mh denotes methyl torsion. Assignment of Bands 2, 5, and 6 as the prominent progression along the DMA torsional coordinate ($\tau_0^2, \tau_0^4, \tau_0^6$; owing to symmetry, transitions are allowed only to even levels in S_1) is confirmed by their (average) inertial defects, -12.3, -11.5, and -11.9 amu Å^2, respectively. All of these values are large in magnitude compared to the ΔI value of the ground state, -7.56 amu Å^2. The data also provide further support for the presence of two minima in the S_1 potential along this coordinate. As one approaches the top of the barrier, $\langle \tau^2 \rangle^{1/2}$ should first decrease and then increase, leading to a zig-zag behavior of ΔI as a function of τ.[25] This is precisely what is

observed. Thus, there must be a maximum at the planar geometry along this coordinate in the S_1 state, if there is a minimum in the S_0 state. The ΔI data also quantitatively support the suggested S_1 barrier height of ~ 190 cm^{-1} along this coordinate since all probed levels lie below this barrier.

Bands 3 and 4, and Bands 7 and 8 also have substantially larger (in magnitude) inertial defects ($\Delta I = -12.5$ and -14.2, and -13.5 and -12.1 amu Å^2, respectively). These values are not only larger than those of the ground state, but they are also larger than the values for the τ^2, τ^4, and τ^6 torsional levels, evidencing substantial displacements along other out-of-plane coordinates. But ambiguities exist concerning the assignments of both pairs of these bands. Saigusa *et al.*[11] assigned Bands 3 and 4 as I_0^2 and $\tau_0^1 M h_0^1$, and Bands 7 and 8 as $\tau_0^2 I_0^2$ and $\tau_0^3 M h_0^1$, but noted that both assignments could be reversed. The torsional levels τ^0 (the zero-point level) and τ^1 should have increasingly negative values of ΔI, compared to the value for τ^2 (-12.3 amu Å^2). Additional activity of the methyl torsional mode should not contribute greatly to ΔI. So, although it is difficult to be certain, the reversed assignment of Band 3 to $\tau_0^1 M h_0$ and Band 4 to I_0^2 seems more reasonable to us. In that event, the value $\Delta I = -14.2$ amu Å^2 seems too large in magnitude to attribute solely to the DMA twist. Additional displacement along the inversion coordinate away from 0^0 would explain the larger value. The barrier to inversion is likely to be quite small. So, the magnitude of the contribution to ΔI from inversion is expected to rise steeply with increasing displacement along this coordinate. For that reason, we are comfortable with the existing assignments of Band 7 as $\tau_0^2 M h_0^2$ (with $\Delta I = -13.5$ amu Å^2) and Band 8 as $\tau_0^3 M h_0^1$ (with $\Delta I = -12.1$ amu Å^2) but more data will be necessary to confirm this conclusion.

C. Methyl group torsional motions

Revealed by the high resolution spectra is additional vibrational motion along the methyl group torsional coordinate of DMABN in its S_1 electronic state. The primary evidence for this motion are the splittings that are observed in the spectra. Each observed high resolution band is split into two or more components, and the different components exhibit different splittings and different relative intensities. Importantly, these relative intensities are independent of backing pressure, showing that they are dictated primarily by the different nuclear spin statistical weights (NSSWs) of the affected levels, not by their relative temperatures, Franck–Condon factors, and/or oscillator strengths. Of the possible feasible tunneling pathways that could be responsible for these NSSWs, inversion of the DMA group would produce two subbands with the same relative intensities, rotation of a single methyl group would produce two subbands with different relative intensities, and (coordinated) rotation of two equivalent methyl groups would produce three or more subbands with different relative intensities. The last possibility is the only one that is consistent with the experimental data.

DMABN is a two-top molecule. In the absence of coupling between the two tops, the effective torsional Hamiltonian is[16]

$$\hat{H}_{\text{eff}}^r = F p_1^2 + (V_3^*/2)(1 - 3 \cos \phi_1) + F p_2^2$$
$$+ (V_3^*/2)(1 - 3 \cos \phi_2), \tag{1}$$

where F is the reduced rotational constant for the motion described by the angles ϕ_1 and ϕ_2, p_1 and p_2 are the angular momenta of the two rotors, and V_3^* is an effective hindering potential. A single methyl rotor governed by a potential of this type has three torsional levels for each torsional quantum number ν, a single A torsional level and two E torsional levels. Degenerate in the infinite barrier limit, the three levels are split by tunneling through a finite barrier (the A–E splitting) and by torsion-rotation interactions (the E-E splitting). A similar situation exists for two equivalent methyl rotors. Here, the original ninefold (3×3) degeneracy is split by tunneling into three groups of levels, labeled by A_1, G, and $E_1 + E_3$. The different levels can be distinguished by their different NSSWs, $\approx 1:2:1$ for $A_1:G:E_1+E_3$ levels. Each of the different subtorsional levels also has its own effective rotational Hamiltonian, since the motions (and the magnitudes of torsion-rotation coupling) that occur in each of the levels are not the same.

In general, the tunneling splitting in different electronic states also is not the same because the potentials governing the torsional motion are not the same. The separations between the A_1, G, and E_1+E_3 levels in each state are expected to be different. Thus, a single band in an electronic spectrum is split into three components; the A_1-A_1 (A) subband, the G-G (G) subband, and the $[(E_1+E_3)–(E_1+E_3)]$ (E) subband. The separations between the subbands are measures of the difference in the V_3^* values in the two states. When all three subbands are observed, the two separations should be equal if the rotors are independent; i.e., if rotor-rotor coupling is small. In favorable cases, these criteria can be used to distinguish rovibrational transitions belonging to one subband from those belonging to another. The separate subbands can be fit using their own, unique rotational Hamiltonians, and the derived values of the torsion-rotation interaction terms can be used to obtain independent estimates of the V_3^* values in both electronic states.

We proceed as follows. First, we note that the different subbands within each band of DMABN can each be identified by differences in their intensities. Next, we note that the different subbands always appear in the same energy sequence; A, G, and E in each band. This means that the three-fold barrier in the S_1 state is less than that in the S_0 state $[V_3^*(S_1) < V_3^*(S_0)]$. Next, we note that only the excited state subtorsional levels G and E are split by the torsion-rotation interaction. D_a, D_b, and D_c are all zero (within experimental error) for the corresponding ground state subtorsional levels. This means that the ground state barrier is on the order of 500 cm^{-1} or more, and that, to a first approximation, the A, G, and E subtorsional levels belonging to $v''=0$ in the ground state are degenerate. This is not a surprising result. The CH$_3$ torsional barrier in the electronic ground state of CH$_3$NH$_2$ is ~ 690 cm^{-1}.[26]

To proceed further, we make several assumptions. We choose $F(S_0)=5.241$ and $F(S_1)=5.285$ cm^{-1} based on *ab initio* calculations. We choose $\rho_a = \cos 30°$ and $\rho_b = \cos 60°$

TABLE V. Methyl group torsional parameters in the ground and electronically excited states of DMABN.

State	Band	D_a, MHz	D_b, MHz	V_3^*, $cm^{-1,a}$	V_3^*, $cm^{-1,b}$	TS, GHz[c]	TS, GHz[d]
S_0	All	~0	~0	>500	543	0	
S_1	2G	42	24	222	230	3	4
-	3G	186	45	153	138	15	18
-	4G	7	0	342	367	0.4	0.5
-	5G	305	28	117	140	14	18
-	6G	118	10	165	180[e]	0.5	9
-	7G	192	37	165	148	12	15
-	8G	554	82	117	107	27	31

[a]Values from D_a obtained from the assigned fit.
[b]Values from GA automated fit.
[c]Experimental tunneling splitting in GHz.
[d]Theoretical tunneling splitting in GHz.
[e]Value from D_a, see text.

since the axes about which the torsional motions are occurring make angles of $\approx \pm 30°$ ($\pm 60°$) with respect to $a(b)$. Note that this assumption is at least qualitatively consistent with the experimental finding that $D_a \gg D_b$ in all perturbed bands. And, since the spacings between the three subbands in each band are approximately equal, we also neglect the possible influence of couplings between the two rotors. We then use Eq. (2) to evaluate the first-order perturbation coefficients $W_{01}^{(1)}$ from the observed values of D_a,[16]

$$D_a = F W_{01}^{(1)} \rho_a. \qquad (2)$$

These coefficients were then used to determine V_3^* from Herschbach's tables.[27] In principle, the values of D_b also should be included in this analysis, but as these are small and much less precise, they were ignored. And, finally, the derived barrier heights were used to compute tunneling splittings that could be compared to the experiment.

Table V lists the values of V_3^* that were derived in this way. The excited state values of V_3^* are all substantially less than that of the S_0 state. The different S_1 vibrational levels have substantially different V_3^* values, varying from 117 to 342 cm^{-1}.

That the excited state values of V_3^* are all substantially less than that of the ground state in DMABN is an extremely important result. Methyl groups attached to "tetrahedral" nitrogen atoms typically have large torsional barriers, of the order of 500 cm^{-1}. Theoretical studies suggest that these large values have their origin in a "hyperconjugative" interaction involving the nitrogen lone pair electrons and the attached methyl group.[28] If this is so, then the substantial decrease in V_3^* values in the excited state of DMABN indicates that the density of lone pair electrons on the nitrogen atom is substantially reduced, compared to the ground state. The (sixfold) CH_3 torsional barrier in the $n \rightarrow 3s$ Rydberg state of CH_3NH_2 is much smaller ($V_6 = 5$ cm^{-1}) (Ref. 29) than the

(threefold) barrier in the ground state ($V_3 = 690$ cm^{-1}),[26] in accord with this thinking. Thus, the smaller values of V_3^* in the S_1 state of DMABN provide firm evidence for charge transfer from the n orbital of nitrogen atom to the π^* orbital(s) of the aromatic ring. Stark effect experiments[30] to determine the dipole moment of S_1 DMABN will provide a more quantitative measure of this effect.

Variations in the V_3^* values among the different S_1 vibrational levels probed in this work may be attributed to several factors. One is the method of fitting the data. Using JB95, we fit the individual subbands separately, obtaining different values of D_a (and D_b) from which the barrier heights were determined separately, as well. In the absence of rotor-rotor coupling, the values for the different subbands belonging to a given ν should be the same. One possible explanation for the fact that they are different is the high uncertainty in the values of D_a for the weaker subbands. Another possible explanation is rotor-rotor coupling. To address this issue, we independently fit all of the subbands together, using the GA method. The Hamiltonian used for this procedure was the full torsion-rotation Hamiltonian, as described by Tan *et al.*,[16] which requires that all torsional subbands with the same ν have the same value of V_3^*. All bands conform to this picture except Band 6, where D_a and the subband separation gives different values of V_3^*. Table V also lists the results of these calculations. Comparing these to experiment, we see that the values obtained by the two different methods agree quite well.

Independent of the possible variations in the V_3^* values within a given ν, the different S_1 vibrational levels of DMABN also have substantially different V_3^* values. They also have very different tunneling splittings (cf. Table V). Substantial coupling between the methyl group torsional motion and other vibrational modes, especially these involving the DMA group, may be responsible for the differences in these values. Motion along one coordinate might strongly facilitate motion along others. Indeed, higher lying S_1 levels have lower V_3^* values, and larger tunneling splittings. The possible disappearance of the $E_1 + E_3$ subbands at higher energy also may be attributed to interactions among these degrees of freedom. Further studies of these effects are in progress.

V. SUMMARY

Summarizing, an extensive study of the electronic spectrum of DMABN at high resolution has revealed information about the properties of the ground and excited states of the isolated molecule. Ground state DMABN is "planar" and less pyramidal; excited (S_1) state DMABN is twisted and more pyramidal, a true TICT state. The spectra also reveal evidence for substantial methyl group torsional activity, a consequence of substantial charge transfer from the nitrogen atom to the ring. Thus, all three vibrational coordinates; DMA torsion, DMA inversion, and methyl group torsion act in concert to "protect" against "back" electron transfer once the photon is absorbed. Thereby created is a stable minimum

on the energy landscape of the S_1 state that is responsible for the unique emissive properties of DMABN and related molecules in the condensed phase.

[1] E. Lippert, W. Lüder, and H. Boos, in the *Proceedings of the Fourth International Meeting on Advances in Molecular Spectroscopy 1959*, edited by A. Mangini (Pergamon, Oxford, 1962), pp. 443–457; see also E. Lippert, W. Lüder, F. Moll, W. Nägele, H. Boos, H. Prigge, and I. Seibold-Blankenstein, Angew. Chem. **73**, 695 (1961).

[2] K. Rotkiewicz, K. H. Grellmann, and Z. R. Grabowski, Chem. Phys. Lett. **19**, 315 (1973); see also Chem. Phys. Lett. **21**, 212(E) (1973).

[3] Early work in this field is comprehensively reviewed by W. Rettig, Angew. Chem., Int. Ed. Engl. **25**, 971 (1986).

[4] K. A. Zachariasse, T. von der Haar, A. Hebecker, U. Leinhos, and W. Kühnle, Pure Appl. Chem. **65**, 1745 (1993).

[5] More recent work is described in Z. R. Grabowski, K. Rotkiewicz, and W. Rettig, Chem. Rev. (Washington, D.C.) **103**, 3899 (2003).

[6] T. Kobayashi, M. Futakami, and O. Kajimoto, Chem. Phys. Lett. **130**, 63 (1986).

[7] E. M. Gibson, A. C. Jones, and D. Phillips, Chem. Phys. Lett. **136**, 454 (1987).

[8] J. A. Warren, E. R. Bernstein, and J. I. Seeman, J. Chem. Phys. **88**, 871 (1988); V. H. Grassian, J. A. Warren, E. R. Bernstein, and H. V. Secor, *ibid.* **90**, 3994 (1989); see also R. D. Gordon, *ibid.* **93**, 6908 (1990); E. R. Bernstein, V. H. Grassian, and J. A. Warren, *ibid.* **93**, 6910 (1990).

[9] O. Kajimoto, H. Yokoyama, Y. Ohshima, and Y. Endo, Chem. Phys. Lett. **179**, 455 (1991).

[10] F. P. Salgado, J. Herbich, A. G. M. Kunst, and R. P. H. Rettschnick, J. Phys. Chem. A **103**, 3184 (1999).

[11] H. Saigusa, N. Miyakoshi, C. Mukai, T. Fukagawa, S. Kohtani, R. Nakagaki, and R. Gordon, J. Chem. Phys. **119**, 5414 (2003).

[12] D. Rappoport and F. Furche, J. Am. Chem. Soc. **126**, 1277 (2004).

[13] J. L. Tomer, K. W. Holtzclaw, L. H. Spangler, and D. W. Pratt, J. Chem. Phys. **88**, 1528 (1988).

[14] W. A. Majewski and W. L. Meerts, J. Mol. Spectrosc. **104**, 271 (1984).

[15] W. A. Majewski, J. F. Pfanstiel, D. F. Plusquellic, and D. W. Pratt, in *Laser Techniques in Chemistry*, edited by A. B. Myers and T. R. Rizzo (Wiley, New York, 1995), p. 101.

[16] X. Q. Tan, D. J. Clouthier, R. H. Judge, D. F. Plusquellic, J. L. Tomer, and D. W. Pratt, J. Chem. Phys. **95**, 7862 (1991).

[17] J. A. Hageman, R. Wehrens, R. de Gelder, W. L. Meerts, and L. M. C. Buydens, J. Chem. Phys. **113**, 7955 (2000).

[18] W. L. Meerts, M. Schmitt, and G. Groenenboom, Can. J. Chem. **82**, 804 (2004).

[19] Described in D. F. Plusquellic, R. D. Suenram, B. Maté, J. O. Jensen, and A. C. Samuels, J. Chem. Phys. **115**, 3057 (2001).

[20] M. J. Frisch, G. W. Trucks, H. B. Schlegel *et al.*, GAUSSIAN 98, Revision A9, Gaussian, Inc., Pittsburgh, PA (1998).

[21] J. L. Tomer, Ph.D. thesis, University of Pittsburgh, 1991.

[22] B. D. Howells, J. McCombie, T. F. Palmer, J. P. Simons, and A. Walters, J. Chem. Soc., Faraday Trans. **88**, 2595 (1992).

[23] W. E. Sinclair and D. W. Pratt, J. Chem. Phys. **105**, 7942 (1996).

[24] G. Berden, J. van Rooy, W. L. Meerts, and K. A. Zachariasse, Chem. Phys. Lett. **278**, 373 (1997).

[25] S. Jagannathan and D. W. Pratt, J. Chem. Phys. **100**, 1874 (1994).

[26] D. Kivelson, J. Chem. Phys. **27**, 353 (1957).

[27] D. R. Herschbach, J. Chem. Phys. **27**, 975 (1957).

[28] See, for example, A. E. Dorigo, D. W. Pratt, and K. N. Houk, J. Am. Chem. Soc. **109**, 6591 (1987).

[29] S. J. Baek, K. W. Choi, Y. S. Choi, and S. K. Kim, J. Chem. Phys. **118**, 11026 (2003).

[30] T. M. Korter, D. R. Borst, C. J. Butler, and D. W. Pratt, J. Am. Chem. Soc. **123**, 96 (2001).